Physics of the Solid State, Vol. 46, No. 10, 2004, pp. 1792–1797. Translated from Fizika Tverdogo Tela, Vol. 46, No. 10, 2004, pp. 1735–1739.
Original Russian Text Copyright © 2004 by Petrov, Balaev, Gokhfel'd, Shaĭkhutdinov, Ospishchev, Aleksandrov.

METALS AND SUPERCONDUCTORS

Crossover from the "Clean" Limit to the "Dirty" Limit in a Network of *S–N–S* Weak Links in $Y_{3/4}Lu_{1/4}Ba_2Cu_3O_7 + BaPb_{1-x}Sn_xO_3$ $(0 \le x \le 0.25)$ Composites

M. I. Petrov, D. A. Balaev, D. M. Gokhfel'd,
K. A. Shaĭkhutdinov, S. V. Ospishchev, and K. S. Aleksandrov
Kirensky Institute of Physics, Siberian Division, Russian Academy of Sciences, Akademgorodok, Krasnoyarsk, 660036 Russia
e-mail: smp@iph.krasn.ru

Received February 5, 2004

Abstract—Composites with a network of "superconductor–normal metal–superconductor" (*S–N–S*) weak links are prepared from a $Y_{3/4}Lu_{1/4}Ba_2Cu_3O_7$ high-temperature superconductor and $BaPb_{1-x}Sn_xO_3$ $(0 \le x \le 0.25)$ metal oxides. It is found that an increase in the tin content x in the nonsuperconducting component of the composite leads to an increase in the electrical resistivity ρ and, hence, to a decrease in the mean free path l of charge carriers. The temperature dependences of the electrical resistivity $\rho(T)$ and critical current $j_C(T)$ of the composites are analyzed in the framework of the de Gennes theory of *S–N–S* junctions. It is demonstrated that the network of weak links in the composites is characterized by a crossover from the "clean" limit $(l \ge L)$ to the "dirty" limit $(l \le L)$ (where L is the effective thickness of N interlayers between high-temperature superconductor grains). *© 2004 MAIK "Nauka/Interperiodica".*

1. INTRODUCTION

It has been universally accepted that, in high-temperature superconducting ceramics, natural grain boundaries forming a Josephson-type weak-link network are responsible for the transport properties of polycrystals. Taking into account disagreement among authors regarding the nature of boundaries (metallic, dielectric, etc.) in polycrystalline high-temperature superconductors [1–12], the inference can be made that their conductivity is governed by technological factors. In our earlier works [5, 10–12], we analyzed the transport properties of polycrystalline high-temperature superconductors with a 1–2–3 structure and conclusively proved that the standard procedure of synthesizing these materials leads to the formation of natural grain boundaries of metallic nature. However, systematic investigations into the preparation and transport properties of polycrystalline high-temperature superconductors with a network of "superconductor–normal metal–superconductor" (*S–N–S*) weak links have been undertaken neither in the "clean" limit (when the mean free path l of charge carriers in the normal metal is greater than the geometric thickness L of N interlayers; i.e., $l \ge L$ [13]) nor in the "dirty" limit ($l \le L$ [13]). In composites based on high-temperature superconductors, the nonsuperconducting component is a material forming boundaries between superconducting grains [6–12, 14–18]. The transport properties of the composite as a whole are governed by the type of nonsuperconducting component (metal [6, 8, 9, 16–18] or dielectric [14, 15]).

Earlier [11], we studied the transport properties of $Y_{3/4}Lu_{1/4}Ba_2Cu_3O_7 + BaPbO_3$ composites. It was shown that these composites have a network of *S–N–S* weak links and that the transport properties of the composites are determined by an N interlayer whose effective thickness L depends on the volume content of the metal. It was established that the experimental temperature dependences of the critical current $j_C(T)$ for the composites are in good agreement with the theoretical dependences $j_C(T)$ for clean *S–N–S* junctions [19]. This made it possible to estimate the effective thickness of N interlayers in the composites under investigation. It turned out that the effective thickness L of N interlayers monotonically increases (in proportion to $V^{1/3}$, where V is the volume content of the nonsuperconducting component) from ~40 Å for the composite with 4 vol % $BaPbO_3$ to ~125 Å for the composite with 45 vol % $BaPbO_3$ [9]. These values of L were used in the present work to make a comparison with the mean free path of charge carriers in the nonsuperconducting component of the composite.

Investigations into the current–voltage characteristics [16] and the critical current [17] of YBCO + $BaPbO_3$ and YBCO + $BaPb_{0.9}Sn_{0.1}O_3$ composites and their analysis in terms of the theory of *S–N–S* junctions [20–23] gave grounds to assert that the network of *S–N–S* junctions is formed in the clean limit for composites containing $BaPbO_3$ and in the effectively dirty limit for composites with $BaPb_{0.9}Sn_{0.1}O_3$. In the authors' opinion, it is of interest to investigate a crossover from the clean limit to the dirty limit in a "high-temperature superconductor + $BaPb_{1-x}Sn_xO_3$" composite by decreasing the conductivity of the $BaPbO_3$ metal oxide through partial replacement of lead by tin ($0 \leq x \leq 0.25$). In this work, we compared the transport properties of composites with the same volume content of the $BaPb_{1-x}Sn_xO_3$ component but with different tin contents x. All the composites were simultaneously prepared according to the same procedure. Therefore, the size distribution of N interlayers can be considered to be identical for all composites of the same series and all changes in the transport properties of the composites thus prepared can be explained by the evolution of the physical properties (in particular, electrical resistance) of the $BaPb_{1-x}Sn_xO_3$ nonsuperconducting component, which is responsible for the formation of weak links between high-temperature superconductor grains.

2. SAMPLE PREPARATION AND EXPERIMENTAL TECHNIQUE

2.1. Synthesis and Electrical Resistivity of $BaPb_{1-x}Sn_xO_3$ Compounds

Compounds $BaPb_{1-x}Sn_xO_3$ at different tin contents x were prepared by solid-phase synthesis from BaO_2, PbO, and SnO_2 oxides at a temperature of 950°C for 160 h with 13 intermediate millings. According to Mössbauer investigations [17], these conditions provide a uniform distribution of tin atoms in the $BaPbO_3$ perovskite structure. The ^{119}Sn Mössbauer spectra of $BaPb_{1-x}Sn_xO_3$ compounds at a tin content $x = 0.1$ are given in [17]. In our experiments, we synthesized a series of samples at tin contents $x = 0$, 0.037, 0.125, and 0.250. The choice of these values of x will be explained below. All the samples were prepared simultaneously. The x-ray powder diffraction patterns of the metal oxides contain only the reflections corresponding to the $BaPbO_3$ structure. The table presents the electrical resistivities ρ of the $BaPb_{1-x}Sn_xO_3$ compounds at temperatures of 5 and 77 K.

An increase in the tin content from 0 to 25 at. % leads to an increase in the electrical resistivity ρ by almost one order of magnitude. Since the structure of the $BaPb_{1-x}Sn_xO_3$ compounds in this case remains virtually unchanged, the electrical resistivity increases as the result of a decrease in the mean free path l of charge carriers [24]. For a $BaPbO_3$ single crystal, the mean free path $l = 220$ Å was obtained by Kitazawa *et al.* [25] from the classical expression

$$l = 3^{1/3}\pi^{2/3}\hbar e^{-2}\rho^{-1}n^{-2/3}, \qquad (1)$$

where $\hbar$ is the Planck constant, e is the elementary charge, and n is the carrier density. It is known that, in $Ba(Pb_{1-x}Bi_x)O_3$ polycrystals, charge scattering by grain boundaries brings about an additional increase in the magnitude of the electrical resistivity ρ [26–28]. Most likely, this increase is the reason why substituting the resistivities ρ of our samples into formula (1) gives underestimated mean free paths (smaller than the lattice constant). In our opinion, it is expedient to calculate the effective mean free path l_{eff}, which depends on the most probable distance r between tin impurity atoms in the structure of the $BaPb_{1-x}Sn_xO_3$ compounds. Taking into account that the mean free path in a polycrystal is shorter than the mean free path in a single crystal, the value of l_{eff} can be calculated from the relationship

$$l_{\text{eff}}^{-1} = l^{-1} + r^{-1}. \qquad (2)$$

Here, $l = 220$ Å for $BaPbO_3$ [25] and the most probable distance r is determined from the formula $r = ax^{-1/3}$ (where x is the atomic fraction of tin; and $a = 4.268$ Å is the lattice constant, which is determined from the x-ray powder diffraction patterns and agrees with the data obtained in [29]). The most probable distances r and the effective mean free paths l_{eff} calculated from the above expressions are listed in the table.

Parameters of $BaPb_{1-x}Sn_xO_3$ nonsuperconducting components of the studied composites

x	ρ(5 K), Ω cm	ρ(77 K), Ω cm	Designation	r, Å	l_{eff}, Å
0	0.0069	0.0057	Sn0	–	220
0.037	0.0085	0.0068	Sn0.037	12.8	12.1
0.125	0.0130	0.0130	Sn0.125	8.5	8.2
0.25	0.0590	0.0537	Sn0.25	4.3	4.2

Note: ρ is the electrical resistivity, r is the most probable distance between Sn atoms, and l_{eff} is the effective mean free path calculated from relationship (2).

2.2. Preparation of Composites Based on a High-Temperature Superconductor and $BaPb_{1-x}Sn_xO_3$ Compounds

The $Y_{3/4}Lu_{1/4}Ba_2Cu_3O_7$ high-temperature superconductor was prepared using the standard procedure. The synthesis of the $BaPb_{1-x}Sn_xO_3$ compounds was described above. The composites were synthesized according to the following procedure, which we called the rapid sintering technique. Powder components of the composite to be synthesized were taken in required proportions, mixed thoroughly in an agate mortar, and pressed into pellets. Then, the pressed pellets in preheated boats were placed in a furnace heated to 930°C and were allowed to stand for 5 min. After high-temperature sintering, the samples were placed in another furnace, held at 400°C for 6 h, and cooled to room temperature together with the furnace. These conditions ensured the recovery of the initial oxygen stoichiometry of high-temperature superconductors with a 1–2–3 structure, because oxygen losses due to sintering are quite probable [30]. By this means, we prepared composites with volume contents $V = 7.5$, 15.0, 30.0, 37.5, and 45.0 vol % $BaPb_{1-x}Sn_xO_3$. Note that the samples with different x and identical V were sintered and saturated with oxygen at the same time. In this work, the composite samples are designated as $S + V$Sn$x$. Here, Snx stands for the nonsuperconducting component (see table). The volume content of the $Y_{3/4}Lu_{1/4}Ba_2Cu_3O_7$ high-temperature superconductor is equal to 100% – V. The x-ray powder diffraction patterns of the composites prepared exhibit only the reflections attributed to the two phases of the initial components. According to electron microscopy, the mean size of high-temperature superconductor grains is approximately equal to 1.5 μm. The superconducting transition temperature determined for the composites from magnetic measurements is equal to 93.5 K. This temperature corresponds to the temperature T_C for the $Y_{3/4}Lu_{1/4}Ba_2Cu_3O_7$ initial high-temperature superconductor.

2.3. Measurements of Transport Properties

The temperature dependences of the electrical resistance $R(T)$ were measured by the standard four-point probe method. These measurements were performed with samples 1.5 × 1.5 × 12 mm in size. The distance between the potential contacts was approximately equal to 10 mm. The electrical resistivity corresponding to the superconducting transition was measured accurate to within $\sim 10^{-6}$ Ω cm. The critical current j_C was determined from the initial portion of the current–voltage characteristic according to a standard criterion of 1 μV/cm [23].

3. RESULTS AND DISCUSSION

3.1. Transport Properties of High-Temperature Superconductor + $BaPb_{1-x}Sn_xO_3$ Composites

Figure 1 shows the temperature dependences of the electrical resistance $R(T)$ of the composites under investigation. The dependences are normalized to the resistance R at $T = 93.5$ K. At this temperature, which coincides with the temperature T_C determined from the magnetic measurements, the electrical resistance exhibits a jump corresponding to the superconducting transition in high-temperature superconductor grains. The second (smooth) portion of the dependence $R(T)$ reflects the transition of weak links to the superconducting state. The temperature T_{C0} at which the electrical resistance disappears strongly depends on the measuring current j. This is characteristic of a weak superconductivity. The influence of the transport current on the dependence $R(T, j)$ was previously studied for other composites prepared by the rapid sintering technique [25–27]. The dependences $R(T)$ shown in Fig. 1 were measured at the current $j = 5$ mA/cm^2 (this current was chosen according to a reasonable signal-to-noise ratio). At weaker currents j, the resistance R does not depend on j. The current–voltage characteristics of all the studied composites, including the S + 45Sn0.25 composite, are nonlinear in the temperature range from T_{C0} to T_C. This is typical of Josephson junctions. The S + 45Snx composites are in a resistive state even at a temperature of 4.2 K. The shift in the threshold of percolation through the superconducting component toward higher superconductor contents in the composites synthesized by the rapid sintering technique was considered in [30, 31].

In [9, 28], it was demonstrated that an increase in the volume content of a metal oxide (in our case, $BaPb_{1-x}Sn_xO_3$) leads to a decrease in the temperature T_{C0} due to an increase in the effective length of metallic weak links. The results of measurements of the electrical resistance at different tin contents x are presented in Fig. 1 in the corresponding panels for each volume content of $BaPb_{1-x}Sn_xO_3$. The influence of the distribution over the geometric parameters of S–N–S junctions in the composites on the electrical resistance is assumed to be identical due to the preparation procedure being the same. Consequently, the decrease in the temperature T_{C0} and variations in the dependences $R(T)$ for a given series of samples depend only on the change in the conductivity of the nonsuperconducting component (or, eventually, on the change in the mean free path of charge carries in the material of N interlayers between high-temperature superconductor grains).

In the S + 37.5Snx composites, an increase in the tin content in the metal oxide to the highest content (x = 0.25) leads to a change in the temperature T_{C0} by ~ 70 K. For composites at a lower content of the metal oxide, the temperature T_{C0} varies over narrower ranges: ~ 30 K for S + 30Snx, ~7 K for S + 15Snx, and ~5 K for S + 7.5Snx. It is known that, with a decrease in the thickness of N interlayers in S–N–S junctions, the effect of their transparency on the superconducting current becomes weaker [13, 19, 23]. This circumstance clearly manifests itself in the temperature dependences of the electrical resistance of the composites.

3.2. Analysis of the Temperature Dependences of the Critical Current for Composites

The nature of weak links can be judged from the temperature dependence of the critical current in a better way than, for example, from the magnitude of the critical current even for a single junction [13, 23, 32, 33] and, especially, for a random network of weak links. The processing of the experimental data for S–N–S junctions in terms of the de Gennes theory [22] makes it possible to evaluate indirectly their physical parameters, such as the mean free path of charge carriers and the geometric thickness of an N interlayer [8, 17, 33–37]. It is expedient to apply this approach to the composites studied in the present work.

At temperatures not far from T_C, the critical current through an S–N–S junction within the de Gennes theory is described by the relationship [22, 23, 35–37]

$$j_C(T) = k(1 - T/T_C)^2 \frac{L/\xi_N}{\sinh(L/\xi_N)}, \quad (3)$$

where k is a constant determined in [22, 23, 35–37]. For a network of S–N–S junctions, the constant k plays the

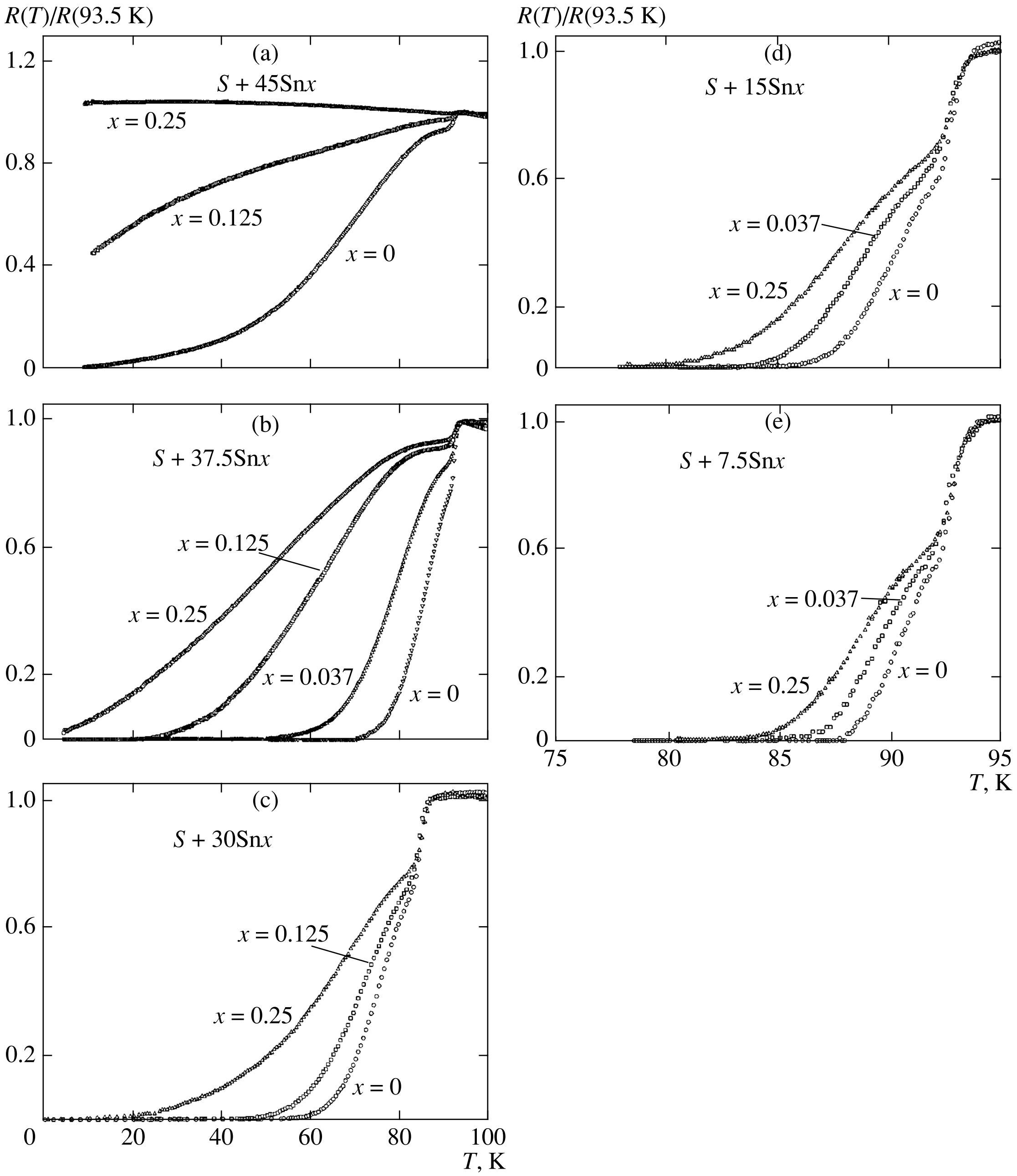

Fig. 1. Temperature dependences of the electrical resistance (normalized to the resistance R at $T = 93.5$ K) for the $S + V\mathrm{Sn}x$ composites at volume contents V = (a) 45.0, (b) 37.5, (c) 30.0, (d) 15.0, and (e) 7.5%.

role of a normalizing factor. In relationship (3), the coherence length ξ_N for a normal metal is determined by the following expressions [35–37]:

$$\xi_N = \hbar V_F / 2\pi k_B T \tag{4}$$

for a clean N interlayer and

$$\xi_N = (\hbar V_F l / 6\pi k_B T)^{1/2} \tag{5}$$

for a dirty N interlayer. In expressions (4) and (5), k_B is the Boltzmann constant and V_F is the Fermi velocity in the normal metal. For $BaPb_{1-x}Sn_xO_3$ compounds, the Fermi velocity V_F was obtained from the relationship $V_F = \hbar 3^{1/3}\pi^{2/3}n^{1/3}m^{-1}$ (where m is the electron mass) at $n = 1.4 \times 10^{20}$ cm^{-3} with the use of the data taken from [25]. In [11], the effective thickness of N interlayers for the 85 vol % $Y_{3/4}Lu_{1/4}Ba_2Cu_3O_7$ + 15 vol % $BaPbO_3$ composite was estimated as $L \sim 100$ Å. These parameters were used to describe the experimental dependences $j_C(T)$, because the composites studied in [11] and in this work were prepared according to the same

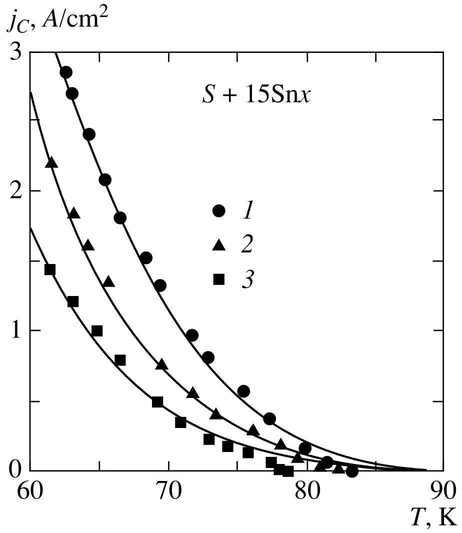

Fig. 2. Experimental temperature dependences of the critical current for the S + 15Snx composites at x = (*1*) 0, (*2*) 0.037, and (*3*) 0.25. Solid lines are the results of the best fitting to the de Gennes theory with the use of formulas (3)–(5) for the effective thickness L = 100 Å and mean free paths l = (*1*) 220, (*2*) 11, and (*3*) 4.2 Å.

procedure. As a result, apart from the normalizing factor, relationship (3) involves a single fitting parameter l.

Figure 2 depicts the experimental temperature dependences of the critical current $j_C(T)$ for S + 15Snx composites and the corresponding curves obtained by fitting to the de Gennes theory. The dependence $j_C(T)$ for the S + 15Sn0 composite in the temperature range 60–80 K was calculated from expressions (3) and (4). The use of expression (4) for the coherence length ξ_N in the case of a composite containing 15 vol % $BaPbO_3$ without impurities is justified because the quantities l (220 Å for $BaPbO_3$ [25]) and L (~100 Å) satisfy the condition for the clean S–N–S junction: $l \geq L$. The solid curves in Fig. 2 approximate the experimental dependences $j_C(T)$ for the S + 15Sn0.037 and S + 15Sn0.25 composites fairly well and represent the results of the best fitting to the de Gennes theory with the use of formulas (3) and (5) for mean free paths l = 11 ± 3 and 4.2 ± 1 Å, respectively. These values are close to the calculated effective mean free paths l_{eff} for $BaPb_{1-x}Sn_xO_3$ compounds (see table). For S + 7.5Snx composites, the experimental dependences $j_C(T)$ are also in good agreement with the theoretical curves calculated from expression (4) for the coherence length $\xi_N(T)$ of the clean N interlayer in the S + 7.5Sn0 sample at L = 80 Å and from expression (5) for the coherence length $\xi_N(T)$ of the dirty N interlayer in the S + 7.5Sn0.25 sample at $l = 4.2 \pm 1$ Å. Therefore, the results of processing of the experimental dependences $j_C(T)$ in terms of the de Gennes theory at temperatures close to T_C indirectly confirm the mean free paths determined above for the $BaPb_{1-x}Sn_xO_3$ compounds (see Subsection 2.1 and table). It can be seen that the inequality $l_{\text{eff}} < L$ (L ~ 80–125 Å) holds for composites with $BaPb_{1-x}Sn_xO_3$ compounds even at x = 0.037. The more strict inequality $l_{\text{eff}} \ll L$ (the diffusive limit [38, 39]) is satisfied at $x \geq 0.125$. Thus, the crossover from the clean limit to the dirty limit in the network of S–N–S weak links in $Y_{3/4}Lu_{1/4}Ba_2Cu_3O_7$ + $BaPb_{1-x}Sn_xO_3$ composites is observed with an increase in the tin content x from 0 to 0.25. In the near future, the results obtained will be described in terms of the theories developed for current–voltage characteristics of S–N–S weak links with a variable mean free path in an N interlayer.

ACKNOWLEDGMENTS

We are grateful to A.D Vasil'ev and A.F. Bovina for performing the x-ray diffraction analysis, O.A. Bayukov for Mössbauer investigations, L.I. Kveglis for electron microscopic examination of the samples, N.I. Kirienko for the assistance in performing the experiments, and S.A. Satsuk and S.I. Popkov for their participation in discussions of the results. M.I. Petrov, and D.M. Gokhfel'd would like to thank R. Kümmel (Universität Würzburg, Germany) for helpful discussions regarding the problem of crossover in S–N–S junctions.

This work was supported in part by the Siberian Division of the Russian Academy of Sciences in the framework of the Lavrent'ev Competition of Research Projects of Young Scientists (2002).

REFERENCES

1. J. Mannhart, P. Chaudhary, D. Dimos, C. C. Tsuei, and T. R. McGuire, Phys. Rev. Lett. **61** (21), 2476 (1988).
2. R. Nicolsky, Cryogenics **29** (3), 388 (1989).
3. J. W. C. De Vries, G. M. Stolmann, and M. A. M. Gijs, Physica C (Amsterdam) **157**, 406 (1989).
4. R. Gross, P. Chaudhari, D. Dimos, A. Gupta, and G. Koren, Phys. Rev. Lett. **64** (2), 228 (1990).
5. M. I. Petrov, S. N. Krivomazov, B. P. Khrustalev, and K. S. Aleksandrov, Solid State Commun. **82** (6), 453 (1992).
6. Z. Damm, T. S. Orlova, B. I. Smirnov, and V. V. Shpeĭzman, Fiz. Tverd. Tela (St. Petersburg) **36** (8), 2465 (1994) [Phys. Solid State **36**, 1341 (1994)].
7. Yu. F. Revenko, A. I. D'yachenko, O. V. Grigut', and V. M. Svistunov, Pis'ma Zh. Tekh. Fiz. **14** (22), 2094 (1988) [Sov. Tech. Phys. Lett. **14**, 909 (1988)].
8. J. J. Calabrese, M. A. Dubson, and J. C. Garland, J. Appl. Phys. **72** (7), 2958 (1992).
9. J. Jung, M. A.-K. Mohamed, I. Isaak, and L. Friedrich, Phys. Rev. B **49** (17), 12188 (1994).
10. M. I. Petrov, D. A. Balaev, B. P. Khrustalev, and K. S. Aleksandrov, Physica C (Amsterdam) **235–240**, 3043 (1994).
11. M. I. Petrov, D. A. Balaev, S. V. Ospishchev, K. A. Shaihutdinov, B. P. Khrustalev, and K. S. Aleksandrov, Phys. Lett. A **237**, 85 (1997).
12. M. I. Petrov, D. A. Balaev, D. M. Gokhfel'd, K. A. Shaĭkhutdinov, and K. S. Aleksandrov, Fiz. Tverd. Tela (St.

Petersburg) **44** (7), 1179 (2002) [Phys. Solid State **44**, 1229 (2002)].

13. K. K. Likharev, Rev. Mod. Phys. **51** (1), 101 (1979).
14. D. Berling, B. Loegel, A. Mehdaouli, S. Regnier, C. Cananoni, and J. Marfaing, Supercond. Sci. Technol. **11**, 1292 (1998).
15. H. Nadifi, A. Ouali, C. Grigoresqu, H. Faqir, O. Monneraau, L. Tortet, G. Vacquier, and C. Boulesteix, Supercond. Sci. Technol. **13**, 1174 (2000).
16. M. I. Petrov, D. A. Balaev, D. M. Gonfeld, S. V. Ospishchev, K. A. Shaihutdinov, and K. S. Aleksandrov, Physica C (Amsterdam) **314**, 51 (1999).
17. M. I. Petrov, D. A. Balaev, S. V. Ospishchev, and K. S. Aleksandrov, Fiz. Tverd. Tela (St. Petersburg) **42** (5), 791 (2000) [Phys. Solid State **42**, 810 (2000)].
18. D. A. Balaev, S. V. Ospishchev, M. I. Petrov, and K. S. Aleksandrov, Supercond. Sci. Technol. **16** (1), 60 (2003).
19. U. Gunsenheimer, U. Schüssler, and R. Kümmel, Phys. Rev. B **49** (9), 6111 (1994).
20. R. Kümmel, U. Gunsenheimer, and R. Nicolsky, Phys. Rev. B **42** (7), 3992 (1990).
21. L. A. A. Pereira and R. Nicolsky, Physica C (Amsterdam) **282–287**, 2411 (1997).
22. P. G. de Gennes, Rev. Mod. Phys. **36**, 225 (1964).
23. A. Barone and J. Paterno, *Physics and Application of the Josephson Effect* (Wiley, New York, 1982; Mir, Moscow, 1984).
24. T. Tsakudo, H. Uwe, T. Suzuki, J. Fujita, J. Shiozawa, and M. Isobe, J. Phys. Soc. Jpn. **55** (1), 314 (1986).
25. K. Kitazawa, A. Katsui, A. Toriumi, and S. Tanaka, Solid State Commun. **52** (4), 459 (1984).
26. Y. Enomoto, M. Suzuki, T. Murakami, T. Inukai, and T. Inamura, Jpn. J. Appl. Phys. **20** (9), L661 (1981).
27. T. D. Thanh, A. Koma, and S. Tanaka, Appl. Phys. **22**, 205 (1980).
28. A. M. Gabovich and D. P. Moiseev, Usp. Fiz. Nauk **150** (4), 599 (1986) [Sov. Phys. Usp. **29**, 1135 (1986)].
29. A. W. Sleight, J. L. Gillson, and P. E. Bierstedt, Solid State Commun. **17** (1), 27 (1975).
30. M. I. Petrov, D. A. Balaev, K. A. Shaihutdinov, and K. S. Aleksandrov, Supercond. Sci. Technol. **14**, 798 (2001).
31. K. A. Shaihutdinov, D. A. Balaev, D. M. Gokhfeld, S. I. Popkov, and M. I. Petrov, J. Low Temp. Phys. **130** (3–4), 347 (2003).
32. U. Schüssler and R. Kümmel, Phys. Rev. B **47**, 2754 (1993).
33. E. Polturak, G. Koren, D. Cohen, E. Aharoni, and G. Deutscher, Phys. Rev. Lett. **67** (21), 3038 (1991).
34. J. Niemeyer and G. von Minngerode, Z. Phys. B **36**, 57 (1979).
35. L. Antogonazza, S. J. Berkowittz, T. H. Geballe, and K. Char, Phys. Rev. B **51** (13), 8560 (1995).
36. K. Char, Physica C (Amsterdam) **282–287**, 419 (1997).
37. L. Antogonazza, B. H. Moeckly, T. H. Geballe, and K. Char, Phys. Rev. B **52** (6), 4559 (1995).
38. V. Barzykin and A. M. Zagoskin, Superlattices Microstruct. **25** (5/6), 797 (1999).
39. P. Dubos, H. Courtois, B. Pannetier, F. K. Wihelm, A. D. Zaikin, and G. Shon, Phys. Rev. B **63**, 064502 (2001).

Translated by O. Borovik-Romanova